

A 2.2GHz Sub-Sampling PLL with 0.16ps_{rms} Jitter and -125dBc/Hz In-band Phase Noise at 700μW Loop-Components Power

Xiang Gao, Eric Klumperink, Gerard Socci*, Mounir Bohsali*, and Bram Nauta

University of Twente, Enschede, The Netherlands; *National Semiconductor, Santa Clara, California
+31-53-489-3811, X.Gao@utwente.nl, B.Nauta@utwente.nl

Abstract

A divider-less PLL exploits a phase detector that directly samples the VCO with a reference clock. No VCO sampling buffer is used while dummy samplers keep the VCO spur <-56dBc. A modified inverter with low short-circuit current acts as a power efficient reference clock buffer. The 2.2GHz PLL in 0.18μm CMOS achieves -125dBc/Hz in-band phase noise with only 700μW loop-components power.

Introduction

Clock multiplication PLLs with very low jitter have recently been proposed based on sub-sampling [1,2] and injection locking [3,4]. In a PLL, the VCO dominates the out-of-band phase noise while the loop-components dominate the in-band phase noise. The sub-sampling (SS) PLL [1,2] can achieve very low in-band phase noise because: 1) divider noise is eliminated; 2) the phase detector (PD) and charge pump (CP) noise is not multiplied by N^2 . This paper describes a new SSPLL design aiming to drastically reduce the loop-components power while maintaining its superior in-band phase noise performance.

Proposed Low Power SSPLL

Fig. 1(a) shows the low power SSPLL architecture. A sub-sampling phase detector (SSPD) samples the VCO with a reference clock Ref and converts VCO phase error into sampled voltage variation. A CP converts the sampled voltage to current. A Pulser controls the CP gain and simplifies the SSPD design to a track-and-hold [1]. A frequency locked loop ensures correct frequency locking and is disabled after locking to save power. In a SSPLL the PD and CP noise contributions are low and thus their power can be scaled down progressively. The VCO and Ref buffers for the SSPD then become the bottlenecks for low power. In [1], they account for 30% and 60% of the total loop-components power, respectively. In this design, we propose two techniques to alleviate these bottlenecks: 1) direct sampling of the VCO without buffer while keeping the disturbance to the VCO low; 2) power efficient Ref buffering with drastically reduced short-circuit current.

Fig. 2 shows the LC VCO and SSPD schematic. Different from [1], no buffer is used between the VCO and SSPD samplers. This saves power as buffers running at f_{VCO} are power consuming. The samplers use PMOS switches since the VCO DC level is high. A concern of this buffer-less direct VCO sampling is the disturbance to the VCO operation. When Ref turns on/off the sampling switch, the VCO is loaded/un-loaded by the sampling capacitors C_{sam} . The VCO load and thus f_{VCO} is changed resulting in binary frequency shift keying (BFSK), causing spurs at integer multiples of f_{ref} . In order to reduce this effect, dummy samplers are added as

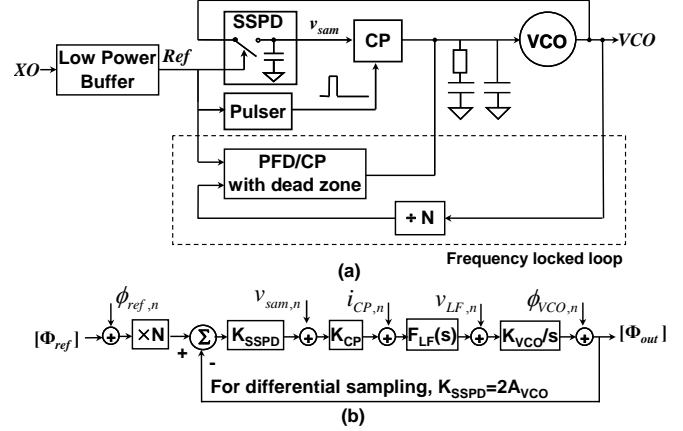


Fig. 1. Sub-Sampling PLL (a) architecture, (b) phase domain model.

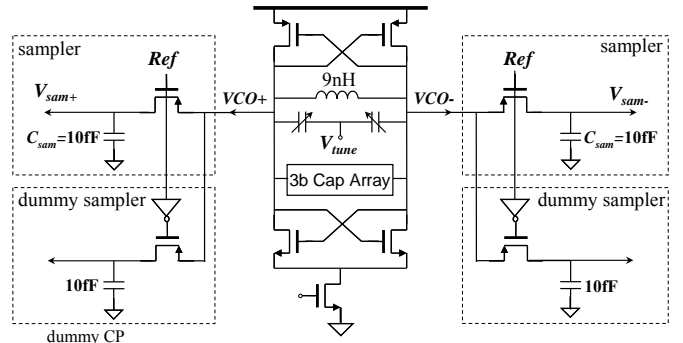


Fig. 2. Schematic of the VCO and SSPD.

shown in Fig. 2, which are controlled by the inverted Ref . A transmission gate (not shown in the figure) compensates the inverter delay. Due to the complementary switching of the sampler and its dummy, the VCO load does not change over time and the BFSK effect is compensated. In reality, the compensation is not perfect due to capacitor mismatch ΔC_{sam} between the sampler and its dummy. Since ΔC_{sam} scales with the value of C_{sam} , it is desirable to have a small C_{sam} for a low spur level. However, a smaller C_{sam} means more sampler noise. With the phase domain model in Fig. 1(b), the in-band phase noise due to the samplers can be derived as

$$\mathcal{L}_{in-band,SSPD} = 10 \log \left(\frac{kT}{2C_{sam} \cdot A_{VCO}^2 \cdot f_{ref}} \right).$$

With $f_{ref}=55\text{MHz}$ and VCO amplitude $A_{VCO}=0.4\text{V}$, C_{sam} is chosen to be 10fF resulting in -136dBc/Hz, 10% of the targeted -126dBc/Hz of [1].

In order to properly sample the GHz VCO, Ref should have a steep sampling edge with a slew rate (SR) higher than the VCO SR. In most applications, Ref is derived from a sine wave crystal oscillator (XO) which often has a much lower SR than the VCO since $f_{ref} \ll f_{VCO}$. A buffer converting the sine XO into a square wave Ref is thus needed. In the 10s-of-MHz frequency range, a CMOS inverter buffer is more power

efficient than a CML buffer as it mainly consumes dynamic power. Noise on Ref is critical for in-band phase noise as it is still multiplied by N^2 when transferred to the SSPLL output; see Fig. 1(b). Thus large inverters need to be used at the expense of power. As the input SR is low and output SR high, power is wasted due to the “short-circuit” current caused by simultaneous conduction of the NMOS and PMOS transistors during switching.

In a sampling process, only one of the two clock edges is used as the sampling edge. In this SSPD design (Fig. 2), the Ref rising edge is the sampling edge. For low noise sampling, the Ref sampling edge is highly critical and needs to be clean while the other Ref edge is not relevant. Fig. 3 shows the proposed Ref buffer, which exploits this property to drastically reduce power. A similar circuit has been used in [2] to control the Ref duty cycle. Here we exploit it to achieve low power. The idea is to directly convey the critical edge and re-position the other non-critical edge at a convenient place to avoid the short-circuit current. The buffer core is an inverter with an NMOS N1 and a PMOS P1. N1 is directly connected to XO as in a conventional inverter, while a timing control circuit (TCC) is inserted between P1 and XO. The TCC consists of two delay cells Δt_1 and Δt_2 and a few standard logic gates. It generates a narrow pulse V_{GP} from the XO and controls the gate of P1. As shown in Fig. 3, Δt_1 and Δt_2 are set such that the time when V_{GP} is low (P1 conducts) and the time when XO is higher than the threshold of N1 (N1 conducts) are non-overlapping. Since f_{ref} is low, this timing plan is easy to achieve. In this way, N1 and P1 will not conduct simultaneously thereby eliminating the short-circuit current. Since the Ref rising edge is the critical sampling edge, the size of N1 is kept big to maintain a low sampling edge noise, while the TCC and P1 use small sizes to save power as they only add noise to the non-critical edge. The first block Inv1 in the TCC is a conventional inverter and has the slow XO as its input. It thus still has short-circuit current, but the contribution to the total buffer power is negligible as its size is small. The proposed buffer thus greatly reduces power while maintaining the critical edge’s noise performance.

Experimental results

The 2.2GHz PLL was fabricated in standard 1.8V 0.18- μ m CMOS with an active area of $0.4 \times 0.5 \text{ mm}^2$ (Fig. 4). Measured in-package with a $1.8V_{pp}$ 55MHz XO as input, the in-band phase noise $\mathcal{L}_{in-band}$ at 200kHz is -125dBc/Hz as shown in Fig. 4. The jitter integrated from 10kHz to 100MHz is 0.16ps_{rms} . The PLL loop-components consume 0.7mW and the VCO 1.8mW. The worst case reference spur measured from 20 chips while changing Ref duty cycle is -56dBc . Fig. 5 summarizes the PLL performance and benchmarks it to low jitter PLLs. This design has the best PLL FOM. Note that we directly used a 55MHz sine-wave XO as the PLL input while [3] used a 50MHz square wave and [4] used a 1GHz sine wave. Compared with [1], the loop-components power is 8x lower while $\mathcal{L}_{in-band}$ is only 1dB worse. Compared with [2], the loop-components power is 3x lower while $\mathcal{L}_{in-band}$ is 4dB better.

References

- [1] X. Gao, et al., “A 2.2GHz 7.6mW sub-sampling PLL with -126dBc/Hz in-band phase noise and 0.15ps_{rms} jitter in 0.18 μ m CMOS,” *ISSCC*, pp. 392 - 393, Feb. 2009.
 [2] X. Gao, et al., “Spur-Reduction Techniques for PLLs Using Sub-Sampling Phase Detection,” *ISSCC*, pp. 474-475, Feb. 2010.

- [3] B. Helal, et al., “A low jitter programmable clock multiplier based on a pulse injection-locked oscillator with a highly-digital tuning loop,” *J. Solid-State Circuits*, pp.1391–1400, May 2009.
 [4] J. Lee and H. Wang, “Study of subharmonically injection-locked PLLs,” *J. Solid-State Circuits*, pp.1539–1553, May 2009.

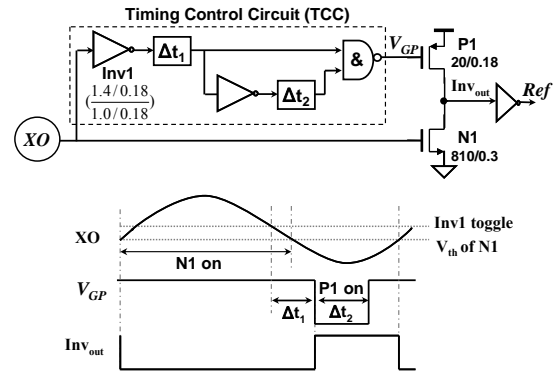


Fig. 3. Schematic and timing diagram of the low power buffer.

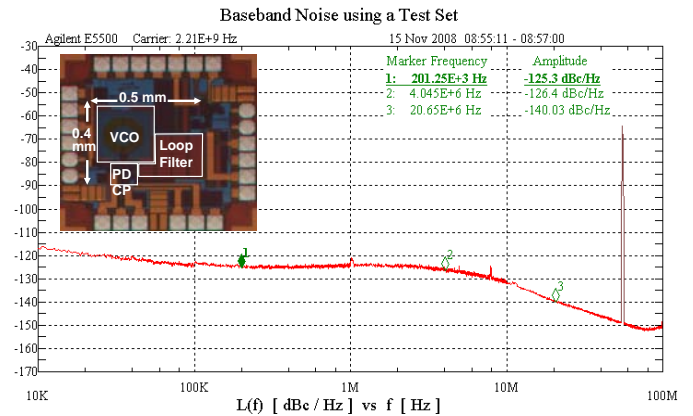


Fig. 4. Measured PLL output phase noise.

	This Work	[1]	[2]	[3]	[4-chip A]	[4-chip B]
f_{out} (GHz)	2.21	2.21	2.21	3.2	20	20
f_{ref} (MHz)	55.25	55.25	55.25	50	1000	2500
RMS jitter σ (ps)	0.16 (10k-100M)	0.15 (10k-40M)	0.3 (10k-100M)	0.13 (100-40M)	0.11 (50k-80M)	0.048 (50k-80M)
In-band phase noise (dBc/Hz)	-125 @200kHz	-126 @200kHz	-121 @200kHz	-127 @1MHz	-113 @1MHz	-123 @1MHz
Ref Spur (dBc) (# of sample)	-56 (#=20)	-46 (#=1)	-80 (#=20)	-64 (#=1)	-46 (#=1)	-55 (#=1)
PLL Power P (mW)	2.5	7.6	3.8	28.6	38	105
Loop-Components Power (mW)	0.7	5.8	2	-	-	-
PLL FOM (dB)	-252	-248	-244	-243	-243	-246
Active area (mm^2)	0.20	0.18	0.20	0.40	<0.45	<0.32
Technology (CMOS)	0.18- μ m	0.18- μ m	0.18- μ m	0.13- μ m	90-nm	90-nm

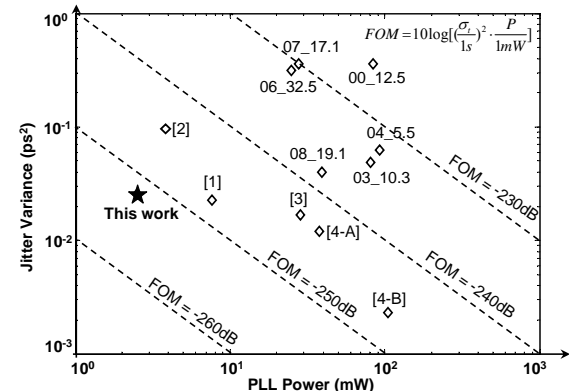


Fig. 5. Performance summary and comparison. The un-referenced ones are the PLL designs with the best FOM in last 10 years’ ISSCC, marked with “Year_PaperNumber”.